

# Overview and Initial Results of the Very Long Baseline Interferometry Space Observatory Programme

H. Hirabayashi,\* H. Hirosawa, H. Kobayashi, Y. Murata, P. G. Edwards, E. B. Fomalont, K. Fujisawa, T. Ichikawa, T. Kii, J. E. J. Lovell, G. A. Moellenbrock, R. Okayasu, M. Inoue, N. Kawaguchi, S. Kamenno, K. M. Shibata, Y. Asaki, T. Bushimata, S. Enome, S. Horiuchi, T. Miyaji, T. Umemoto, V. Migenes, K. Wajima, J. Nakajima, M. Morimoto, J. Ellis, D. L. Meier, D. W. Murphy, R. A. Preston, J. G. Smith, S. J. Tingay, D. L. Traub, R. D. Wietfeldt, J. M. Benson, M. J. Claussen, C. Flatters, J. D. Romney, J. S. Ulvestad, L. R. D'Addario, G. I. Langston, A. H. Minter, B. R. Carlson, P. E. Dewdney, D. L. Jauncey, J. E. Reynolds, A. R. Taylor, P. M. McCulloch, W. H. Cannon, L. I. Gurvits, A. J. Mioduszewski, R. T. Schilizzi, R. S. Booth

High angular resolution images of extragalactic radio sources are being made with the Highly Advanced Laboratory for Communications and Astronomy (HALCA) satellite and ground-based radio telescopes as part of the Very Long Baseline Interferometry (VLBI) Space Observatory Programme (VSOP). VSOP observations at 1.6 and 5 gigahertz of the milli-arc-second-scale structure of radio quasars enable the quasar core size and the corresponding brightness temperature to be determined, and they enable the motions of jet components that are close to the core to be studied. Here, VSOP images of the gamma-ray source 1156+295, the quasar 1548+056, the ultraluminous quasar 0014+813, and the superluminal quasar 0212+735 are presented and discussed.

The angular resolution that is achievable with interferometric techniques is superior to the angular resolution that is achieved with other methods in astronomy. VLBI observations involve a number of widely spaced radio telescopes that simultaneously observe a celestial radio source ( $I$ ). The angular resolution  $\theta$  of a VLBI observation can be approximated by  $\theta = \lambda/D$ , where  $\lambda$  is the observing wavelength and  $D$  is the longest projected baseline (perpendicular to the source direction) that was sampled in the observation. The coherent combination of signals from two separate telescopes produces interference fringes in a similar manner to Young's double-slit experiment in optics. Sampling a wide range of baseline lengths and orientations with a larger number of telescopes allows the structure of radio sources to be imaged on milli-arc second (mas) scales (2). For ground-based VLBI experiments, the longest projected baselines are limited to  $\sim 10,000$  km, which does not allow observers to distinguish fine-scale structure in many radio sources.

To lengthen VLBI baselines, an orbiting radio telescope was launched to co-observe radio sources with ground-based arrays of

radio telescopes. VSOP is a complex international endeavor involving a global network of  $\sim 40$  radio telescopes, five tracking stations, and three data-correlating facilities. Simultaneous observations with HALCA's 8-m-diameter radio telescope and ground-based radio telescopes create a radio telescope that is up to three times as large as ground-based VLBI arrays (Fig. 1), and here we present some examples of the detailed images that the extended VLBI network can provide.

## The Satellite

The second Mu Space Engineering Satellite (MUSES-B) was launched on 12 February 1997. After its launch, the satellite was renamed HALCA. HALCA was placed in an orbit inclined by  $31^\circ$  to Earth's equator with an apogee of 21,400 km above Earth's surface, a perigee height of 560 km, and an orbital period of 6.3 hours.

HALCA's radio telescope has a main reflector with an effective diameter of 8 m (3). The telescope uses Cassegrainian optics, with a hexagonal subreflector inscribed in a 1.1-m-diameter circle. Radio waves are focused by the reflectors into a 2.5-m-long feed horn. Near the throat of the feed horn, a separate

coupler for each observing band couples the left-circular-polarized part of the received signal to a transmission line for transfer to low-noise amplifiers (4).

The standard observing mode uses two 16-MHz base-band channels (each channel is 2-bit sampled at the Nyquist rate of 32 megasamples per second) generating data at 128 megabits per second. Data are transmitted to the ground in real time at 14.2 GHz by a 45-cm link antenna. The ranges of the three observing bands are 1.60 to 1.73, 4.7 to 5.0, and 22.0 to 22.3 GHz. Early in HALCA's in-orbit checkout, it was discovered that the performance at 22 GHz was impaired and that routine observing at 22 GHz was not possible.

HALCA can make observations only when its solar panels are fully illuminated and when two-way communications with one of the five tracking stations can be maintained. Observations of radio sources within  $70^\circ$  of the sun are not possible because the main antenna shadows the solar panels. Observing with HALCA is halted when the sun

H. Hirabayashi, H. Hirosawa, H. Kobayashi, Y. Murata, P. G. Edwards, E. B. Fomalont, K. Fujisawa, T. Ichikawa, T. Kii, J. E. J. Lovell, G. A. Moellenbrock, and R. Okayasu are with the Institute of Space and Astronautical Science, Sagamihara, Kanagawa 229-8510, Japan. M. Inoue, N. Kawaguchi, S. Kamenno, K. M. Shibata, Y. Asaki, T. Bushimata, S. Enome, S. Horiuchi, T. Miyaji, and T. Umemoto are with the National Astronomical Observatory, Mitaka, Tokyo 181-8588, Japan. V. Migenes is with the National Astronomical Observatory, Mitaka, Tokyo 181-8588, Japan, and the University of Guanajuato, Guanajuato, CP 36000, Mexico. K. Wajima is at Ibaraki University, Mito, Ibaraki, 310-8512 Japan. J. Nakajima is with the Communications Research Laboratory, Kashima, Ibaraki 314-0012, Japan. M. Morimoto is at Kagoshima University, Kagoshima 890-0064, Japan. J. Ellis, D. L. Meier, D. W. Murphy, R. A. Preston, J. G. Smith, S. J. Tingay, D. L. Traub, and R. D. Wietfeldt are with the Jet Propulsion Laboratory, 4800 Oak Grove Drive, Pasadena, CA 91109, USA. J. M. Benson, M. J. Claussen, C. Flatters, J. D. Romney, and J. S. Ulvestad are with the National Radio Astronomy Observatory, Socorro, NM 87801, USA. L. R. D'Addario, G. I. Langston, and A. H. Minter are with the National Radio Astronomy Observatory, Green Bank, WV 24944, USA. B. R. Carlson and P. E. Dewdney are with the Dominion Radio Astrophysical Observatory, Herzberg Institute of Astrophysics, National Research Council of Canada, Penticton, British Columbia V2A 6K3, Canada. D. L. Jauncey and J. E. Reynolds are with the Australia Telescope National Facility, Epping, New South Wales 2122, Australia. A. R. Taylor is at the University of Calgary, Calgary, Alberta, T2N 1N4, Canada. P. M. McCulloch is at the University of Tasmania, Hobart, Tasmania 7000, Australia. W. H. Cannon is with the Center for Research in Earth and Space Technology/York University, Ontario, M3J 3K1 Canada. L. I. Gurvits is with the Joint Institute for VLBI in Europe, 7991 PD Dwingeloo, Netherlands, and the Astro Space Center, P.N. Lebedev Physical Institute, Moscow 117810 GSP-1, Russia. A. J. Mioduszewski is with the Joint Institute for VLBI in Europe, 7991 PD Dwingeloo, Netherlands, and the National Radio Astronomy Observatory, Socorro, NM 87801, USA. R. T. Schilizzi is with the Joint Institute for VLBI in Europe, 7991 PD Dwingeloo, Netherlands. R. S. Booth is with the Onsala Space Observatory, Chalmers University of Technology, S-43992 Onsala, Sweden.

\*To whom correspondence should be addressed. E-mail: hirax@vsop.isas.ac.jp

is eclipsed by Earth or the moon and during periods when communication with a tracking station is not possible. Two Ni-Cd batteries are used to provide a backup power supply

and to power the satellite during eclipses. Observations have typical durations of 10 hours with, generally, one radio source observed per day.

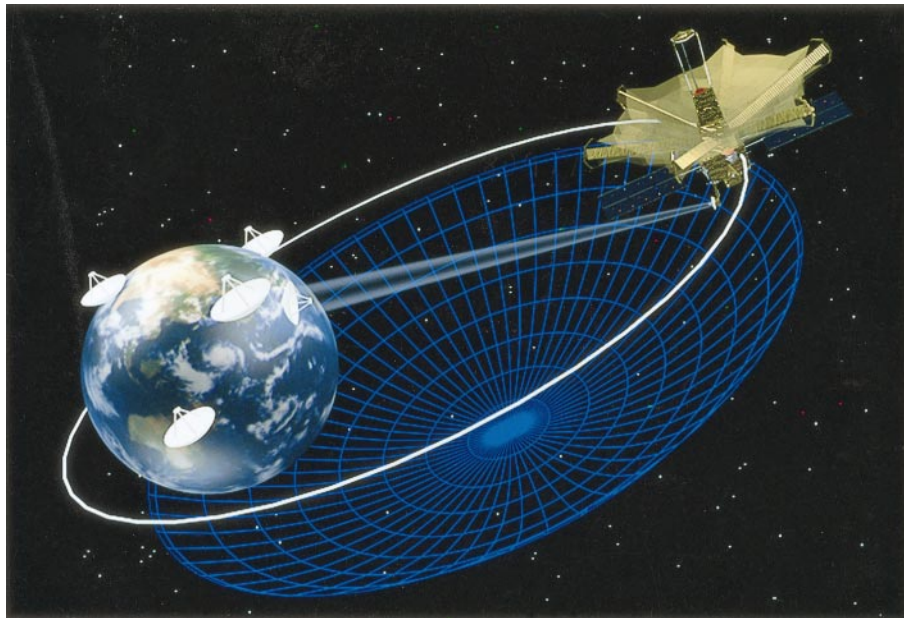


**Fig. 1.** An artist's impression of HALCA co-observing with ground-based radio telescopes to create a radio telescope that is much larger than that achievable on Earth only.

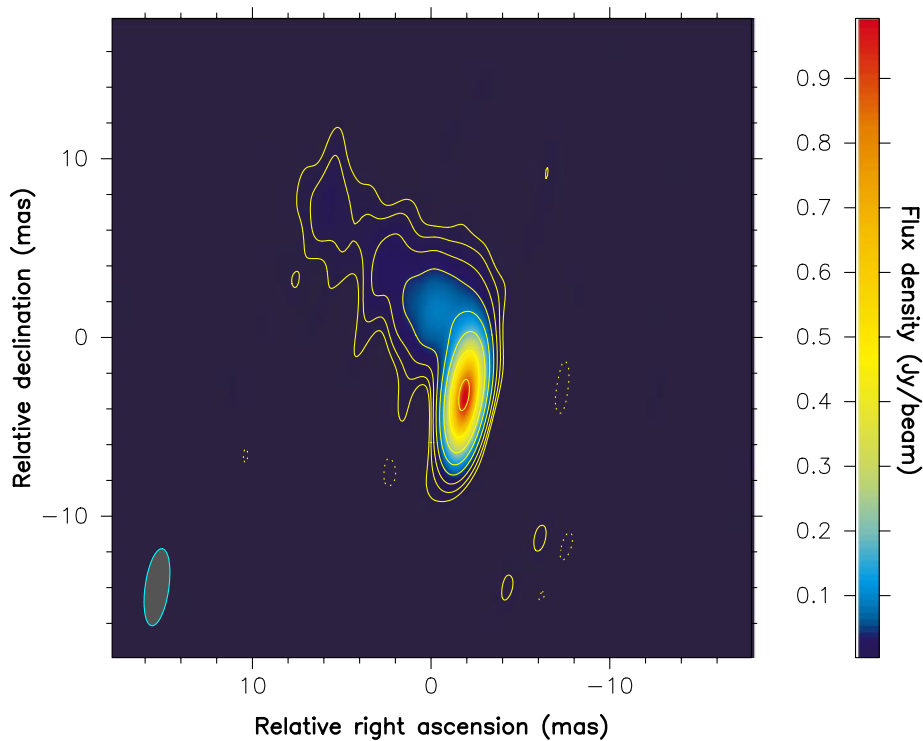


**Fig. 2.** A 1.6-GHz image of the quasar 1156+295 made from observations with HALCA (using the Green Bank tracking station) and the VLBA. The synthesized beam of 4.4 mas by 1.4 mas [full width at half maximum (FWHM)] at a position angle of  $-8.9^\circ$  is shown at the bottom left of the figure. The scale at the right shows the flux density in janskys per beam. The root mean square (rms) residual noise level in the image is 2.5 mJy per beam. The contours are at  $-1$  (dashed lines in Figs. 1 through 4), 1, 2, 4, 8, 16, 32, 63, and 128 times 7 mJy per beam. At the distance of the quasar, 1 mas corresponds to 17.5 light-years.

The sensitivity of a radio telescope may be characterized by its antenna gain and its system noise temperature. The gain of a radio telescope is normally measured in terms of the increase in system noise temperature (in kelvin) per unit flux density (in janskys, where  $1 \text{ Jy} = 10^{-26} \text{ W m}^{-2} \text{ Hz}^{-1}$ ) of a source. For HALCA, the observations of the calibration source Cygnus A (5) resulted in gains of  $0.0043 \text{ K Jy}^{-1}$  at 1.6 GHz and  $0.0062 \text{ K Jy}^{-1}$  at 5 GHz (corresponding to 24 and 35% efficiencies for an effective 8-m-diameter reflector). The lower gain at 1.6 GHz is due in part to diffraction losses that were caused by the limited size of the subreflector, which was constrained by the size of the rocket nose fairing.

The system noise temperature is determined by adding to the receiver input the signal from a diode noise generator, the output of which was calibrated against fundamental noise standards before launch. HALCA's receivers are not cryogenically cooled, resulting in typical system temperatures of 75 K at 1.6 GHz and 95 K at 5 GHz. The overall sensitivity is the ratio of gain to noise temperature, which is conventionally inverted to give 17,400 Jy at 1.6 GHz and 15,300 Jy at 5 GHz, with uncertainties of 10%.

### Tracking, Correlation, and Data Processing

To observe radio sources with HALCA, we must establish a two-way time transfer link between the satellite and a ground tracking station; the tracking station transmits the reference signal derived from its hydrogen maser and receives and records the digitized astronomical signal from the satellite (6). Five dedicated tracking stations, located at Usuda (Japan), Goldstone (CA, USA), Green Bank (WV, USA), Robledo (Spain), and Tidbinbilla (Australia), are used for the VSOP mission (7).

The correlation of ground-based VLBI data has become relatively routine (1). However, the correlation of VSOP data is more complex, requiring two additional sets of information: (i) the precise reconstructed orbit of HALCA and (ii) a series of time corrections that are produced by each tracking station. Results indicate that reconstructed orbits with root sum square errors of 15 m in position and  $6 \text{ mm s}^{-1}$  in velocity can be obtained (8). The remaining uncertainty is handled by allowing for a suitable range of positions and velocities of the satellite during correlation.

The detection of signals from weak radio sources is aided by integrating, or coherently combining, the correlator output data over a period that is much longer than the typical correlator output period of several seconds. The maximum integration time is limited by uncorrected phase variations in the link to the

satellite. Measurements made from correlations of VSOP data show that data can be integrated for up to 5 min at 1.6 and 5 GHz with an acceptably small loss of coherence, provided that the time corrections measured at the tracking stations are properly applied. Without such corrections, the integration time limit would be  $\sim 30$  s, preventing the detection of many weaker sources.

### VSOP Observations

About 30% of HALCA's 3- to 5-year in-orbit time is used for observing extragalactic radio sources such as quasars, radio galaxies, and BL Lacertae objects. Observations of hydroxyl masers and pulsars at 1.6 GHz are also being made. About 15% of the in-orbit time is devoted to the VSOP Survey Program, which is a mission-led systematic survey of active galactic nuclei. The survey observations are generally of a shorter duration and are made with fewer telescopes than the other observations. Nevertheless, the VSOP Survey Program should provide a large complete sample of homogeneous data on sub-milli-arc-second radio structures, which is essential for studying cosmology and the statistics of active galactic nuclei (AGN).

*The gamma-ray source 1156+295.* A 1.6-GHz image (Fig. 2) of the quasar 1156+295 was obtained from a 2.7-hour observation using the 10-element Very Long Baseline Array (VLBA) and HALCA on 4 June 1997. The redshift of 0.729 measured for this source (9) corresponds to a distance of 6.3 billion light-years from Earth (10). The quasar has a compact bright core and an extended milli-arc-second-scale jet on one side of the core. The standard physical model for this structure predicts that the core contains a massive black hole and that symmetric relativistic jets, powered by accretion onto the black hole, are ejected from this core. In most cases, only the jet moving toward us is seen, because of substantial Doppler boosting (11, 12).

The jet bends within a few milli-arc seconds of the core (Fig. 2). Previous ground-based VLBI observations have provided evidence of motions apparently greater than the speed of light (superluminal motion) for the jet components in 1156+295, which is interpreted as an illusion caused by the relativistic motion of plasma close to the line of sight (13). The pronounced bend close to the core may be a consequence of the small angle to the line of sight, as projection effects exaggerate small bends in such cases.

The quasar 1156+295 has been detected as a source of  $>100$  MeV gamma rays (14). Many of the brightest, most compact radio-loud AGN have been identified with  $>100$  MeV gamma-ray sources. However, many sources with similar radio properties have not been detected at gamma-ray energies, and

VSOP observations are exploring the differences between gamma-ray-loud and gamma-ray-quiet quasars.

One difference between the gamma-ray-loud and gamma-ray-quiet classes appears to be in the distributions of their brightness temperatures (15). The surface brightness of a radio source is conveniently represented by brightness temperature. Spectral studies have established that extragalactic radio sources emit nonthermal synchrotron radiation from highly relativistic electrons gyrating in magnetic fields. The brightness temperature of a synchrotron radio source corresponds to the temperature of an equivalent blackbody that produces the same amount of radiation in the same solid angle at the same observing frequency.

There is a brightness temperature limit of  $\sim 10^{12}$  K for incoherent synchrotron emission in the rest frame of the emitting plasma. Above this limit, the energy losses due to inverse Compton scattering (in which the synchrotron-emitting electrons lose energy by scattering photons to higher energies) become catastrophic, and the source rapidly "cools" to  $10^{11}$  to  $10^{12}$  K (16). The brightness temperature observed in our reference frame differs from its value in the emitted frame by the factor  $\delta/(1+z)$ , where  $\delta$  is the Doppler factor (12) of the component in the rest frame of the radio source core and  $z$  is the source redshift.

The core brightness temperature in the source frame of 1156+295, which is derived by model-fitting the VSOP data, is  $0.5_{-0.4}^{+1.0} \times 10^{12}$  K under the assumption that the source has a Gaussian brightness profile. Models that are more realistic, such as an optically thin sphere with uniform emissivity or an optically thick sphere, result in derived brightness temperatures that are 0.43 and 0.36 times the brightness temperatures of the Gaussian model, respectively. Because 1156+295 has a brightness temperature of  $<10^{12}$  K, brightness temperature arguments do not require relativistic beaming in the core, although the superluminal motion of the jet components implies relativistic beaming in the jet.

*The stationary component in 1548+056.* A 1.6-GHz VSOP image (Fig. 3) of the quasar 1548+056 [ $z = 1.422$  (17), corresponding to a distance of 9.3 billion light-years from Earth (10)] was obtained from an 8-hour observation with the 6 m by 22 m Australia Telescope Compact Array (Narrabri, Australia), the University of Tasmania 26-m telescope (Hobart, Australia), the Tidbinbilla 70-m telescope, the Usuda 64-m telescope, the Shanghai 26-m telescope (China), and HALCA on 20 August 1997. The simplest interpretation of the image is that the higher-flux-density component is the core. However, at these frequencies, the synchrotron radiation from the core can be self-absorbed, with the synchrotron-emitting electrons absorbing

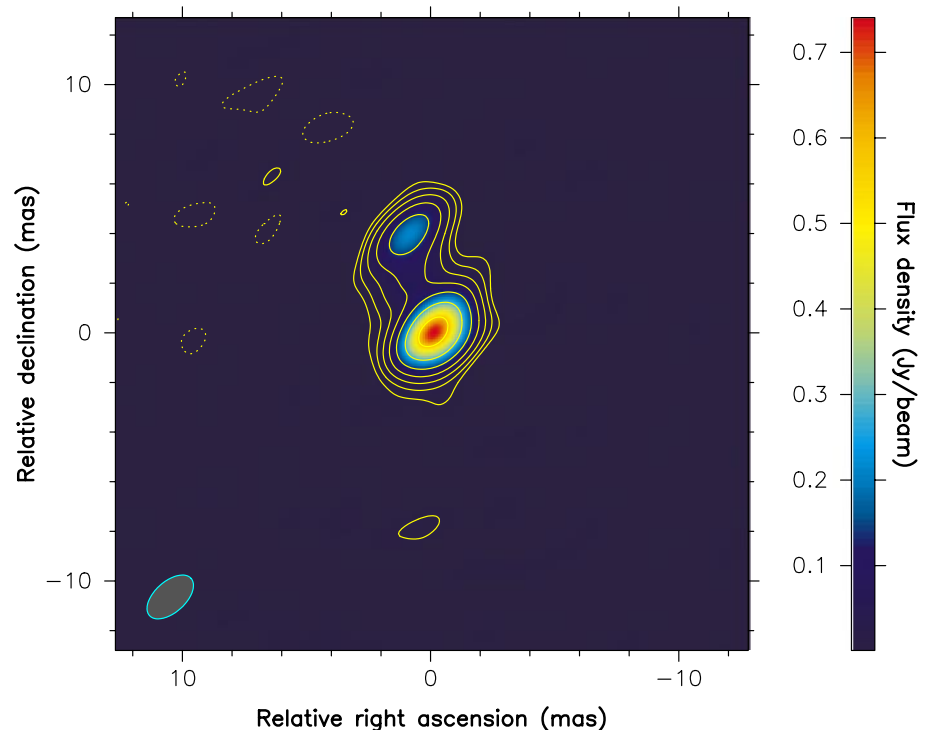


**Fig. 3.** A 1.6-GHz image of the quasar 1548+056 made from an observation with HALCA (using the Goldstone and Usuda tracking stations) and from telescopes in Australia, China, and Japan. The synthesized beam is 2.3 mas by 1.3 mas (FWHM) at a position angle of  $-48.2^\circ$ . The residual noise level in the image is 3.6 mJy per beam (rms). The contours are at  $-1, 1, 2, 4, 8, 16, 32,$  and  $64$  times 9 mJy per beam. At the distance of the quasar, 1 mas corresponds to 18.6 light-years.

the radio photons, and the core only becomes evident at higher frequencies. Ground-based observations at 5 (18) and 15 GHz (19) show that the relative strength of the high-flux-density component increases with increasing frequency, confirming that this is the flatter-spectrum core and that the region of lower flux density is a steeper-

spectrum component in the jet.

A comparison with ground-based images at other frequencies indicates that the lower-flux-density component has shown no discernible motion over the past 12 years (20). One interpretation of this phenomenon, also observed in some other sources, is that the jet is ejected from the core at an appreciable

angle to the line of sight but that the stationary component corresponds to a region where the jet bends toward the line of sight and the radiation is Doppler boosted at this point (21). Alternatively, such features have been explained by stationary shocks in the underlying jet flow (22).

*The ultraluminous high-redshift quasar 0014+813.* With  $z = 3.366$  (23), 0014+813 is one of the most luminous quasars known and is at a distance of 13.6 billion light-years from Earth (10). An observation with the x-ray satellite ASCA (the Advanced Satellite for Cosmology and Astrophysics) has led to the conclusion that, unlike other x-ray-detected high-redshift quasars, 0014+813 exhibits higher absorption than could be attributed to intervening matter in our galaxy (24). The estimated excess absorption, corresponding to a column density of hydrogen of about  $13.4 \times 10^{20} \text{ cm}^{-2}$ , is thought to be intrinsic to the quasar because there is no evidence for any intermediate absorption between our galaxy and 0014+813 (25). These facts suggest a geometry with the axis of the radio jet being widely separated from the line of sight and the excess absorption occurring in material surrounding the core. Such a scenario would imply that highly beamed radio emission is unlikely, unless the compact radio structure of the source is bent. This hypothesis can only be checked by VLBI observations at gigahertz frequencies with better angular resolution than that afforded by ground-based observations.

A 1.6-GHz image (Fig. 4) of 0014+813 shows a well-resolved core-jet structure, with ground-based VLBI images confirming the highest-flux-density component as the core (26). This VSOP observation was made over 8 hours on 16 September 1997 with HALCA, six telescopes of the European VLBI Net-

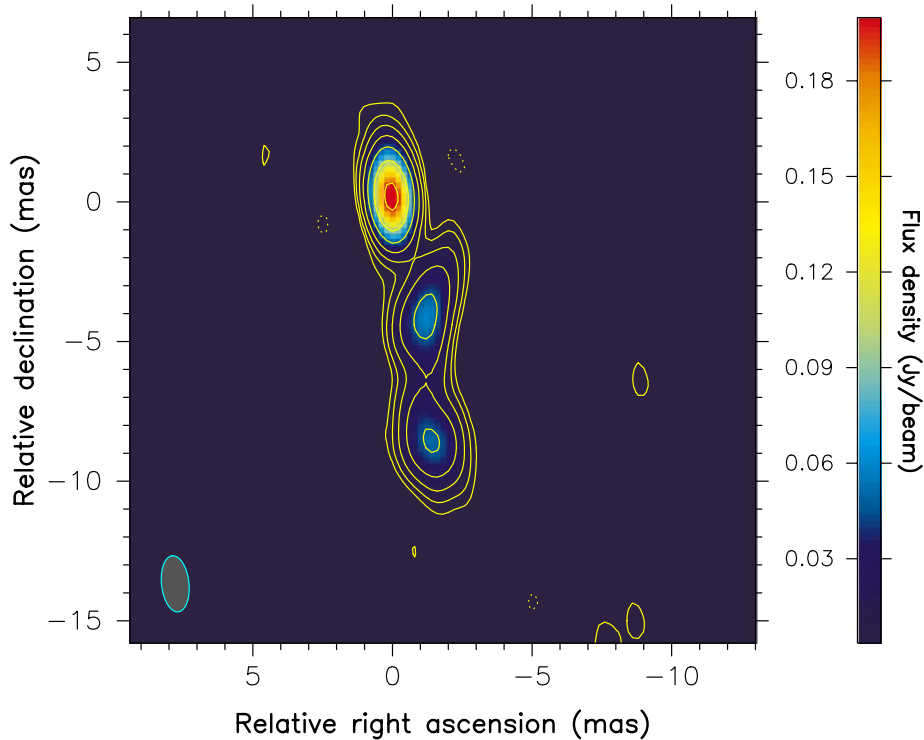
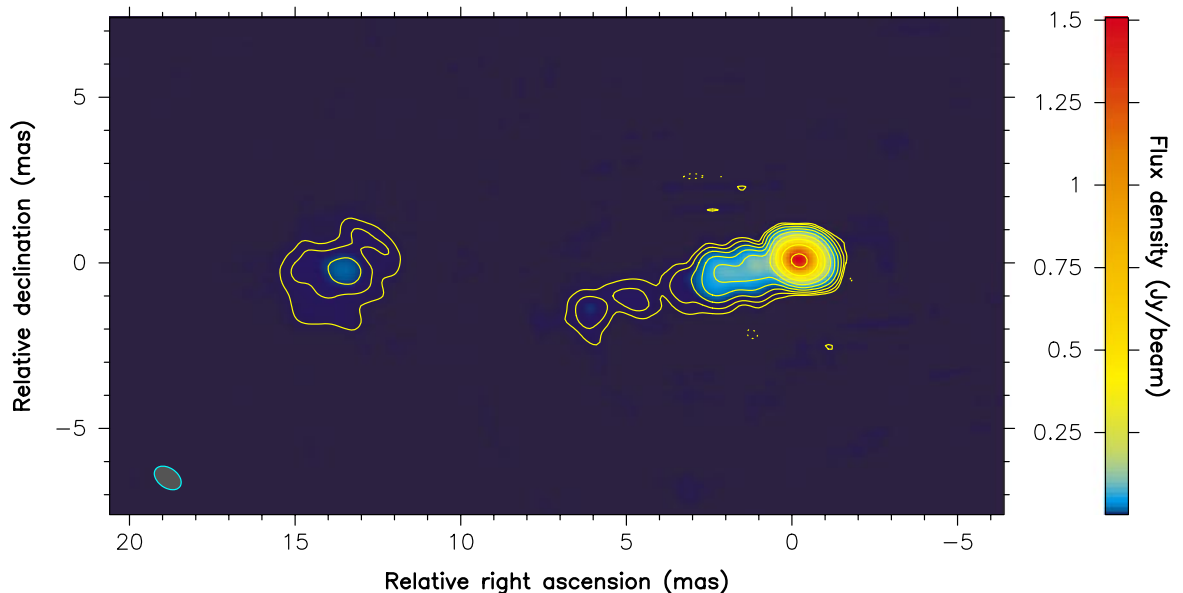


**Fig. 4.** A 1.6-GHz image of the high-redshift quasar 0014+813 made from an observation on 16 September 1997 with HALCA (using the Goldstone, Green Bank, and Tidbinbilla tracking stations), telescopes of the European VLBI Network, and the Green Bank 43-m telescope. The synthesized beam is 2.0 mas by 0.98 mas (FWHM) at a position angle of  $6.2^\circ$ . The residual noise level in the image is 0.9 mJy per beam (rms). The contours are at  $-1, 1, 2, 4, 8, 16, 32,$  and  $64$  times 3 mJy per beam. At the distance of the quasar, 1 mas corresponds to 15.1 light-years.

**Fig. 5.** A 5-GHz image of the quasar 0212+735 made from an observation on 6 September 1997 with HALCA (using the Green Bank and Goldstone tracking stations) and the VLBA. The synthesized beam is 0.9 mas by 0.6 mas (FWHM) at a position angle of  $57.0^\circ$ . The noise level in the image is 0.9 mJy per beam (rms), and the contours levels are  $-1, 1, 2, 4, 8, 16, 32, 64, 128,$  and  $256$  times 5 mJy per beam. At the distance of the quasar, 1 mas corresponds to 17.1 light-years.



work [the Effelsberg 100-m telescope (Germany), the Jodrell Bank 76-m telescope (England), the Noto 32-m telescope (Italy), the Onsala 25-m telescope (Sweden), the Torun 32-m telescope (Poland), and the Westerbork 25-m telescope (Netherlands)] and the National Radio Astronomy Observatory (NRAO) Green Bank 43-m telescope. Contrary to expectations from the x-ray data, the one-sided VLBI jet morphology is consistent with a small to moderate angle to the line of sight for the radio jet axis (27), requiring further investigation into the unexpected excess absorption at x-ray energies.

*The superluminal quasar 0212+735.* A 5-GHz image (Fig. 5) of the quasar 0212+735 [ $z = 2.367$  (28)], corresponding to a distance of  $\sim 12$  billion light-years from Earth (10)] was obtained from a 14-hour observation on 6 September 1997 with HALCA and the VLBA. A comparison of the image with previous images from ground-based observations reveals that the components at 2.1 and 6.3 mas from the core can be identified with components [designated as C2 and C3, respectively (29)] that were observed over the past 15 years (29, 30). It was reported that C2 is moving away from the core with an apparently superluminal speed of  $(4.0 \pm 2.2)h^{-1}$  times the speed of light (29), where  $h$  is the scaling factor used when Hubble's constant  $H$  is expressed as  $100h \text{ km s}^{-1} \text{ Mpc}^{-1}$ . A comparison of the 1985 epoch (29) with the VSOP image yields component speeds of  $(2.8 \pm 1.0)h^{-1}$  and  $(3.0 \pm 1.0)h^{-1}$  times the speed of light for C2 and C3, respectively, establishing that C3 is also displaying superluminal motion. The bright feature  $\sim 14$  mas from the core was also evident 15 years ago, but it does not appear to display the same apparent speed as the other components, although determining the motion of such an extended feature is a difficult task.

## Discussion

These observations demonstrate that space VLBI can clearly resolve the individual components in the jets of quasars and can discern bends in the jet close to the core. These observations will improve our understanding of the physical nature of jet components, showing whether they are due to bulk motion of discrete components or whether they reflect the "pattern speed" of shocks propagating along the jet. In

particular, matched resolution images, which combine VSOP observations at a given frequency with ground observations at a frequency about three times higher, allow the spectral characteristics of the core and jet components to be inferred, with implications for the nature of the individual components and their environment (31). Brightness temperatures are another means of probing the nature of compact radio sources. The brightness temperatures of the strongest compact sources determined at gigahertz frequencies with the finest resolution obtainable from ground-based interferometry are, coincidentally,  $\sim 10^{12}$  K, which is similar to the inverse Compton limit. A number of sources (15, 32) were found to have source frame brightness temperatures  $> 10^{12}$  K. These brightness temperatures were interpreted as being due to bulk relativistic motion close to the line of sight, with the inferred Doppler factors being consistent with those determined from superluminal motion studies (32). Measurements of brightness temperatures on Earth-space baselines, a primary aim of the VSOP Survey Program, will be of great importance in determining whether the  $10^{12}$  K cutoff is approached in the cores of extragalactic radio sources or whether, as has been suggested, some mechanism prevents radical departures from minimum energy and equipartition in these objects (33). Especially interesting will be the comparison of Doppler factors that are derived from core brightness temperature measurements with factors that are estimated from core variability and jet component motions.

## References and Notes

1. A. R. Thompson, J. M. Moran, G. W. Swenson, *Interferometry and Synthesis in Radio Astronomy* (Wiley, New York, 1986).
2. One milli-arc second ( $2.78 \times 10^{-7}$  degrees) is about the angle spanned by a strand of hair at a distance of 20 km from the observer.
3. H. Hirasawa and H. Hirabayashi, *Space Technol.* **16** (no. 3), 161 (1996).
4. H. Hirabayashi et al., in preparation.
5. J. W. M. Baars, R. Genzel, I. I. K. Pauliny-Toth, A. Witzel, *Astron. Astrophys.* **61**, 99 (1977).
6. L. R. D'Addario, *IEEE Trans. Instrum. Meas.* **40**, 584 (1991); N. Kawaguchi et al., in *VLBI Technology: Progress and Future Observational Possibilities*, T. Sasao, S. Manabe, O. Kameya, M. Inoue, Eds. (Terra Scientific, Tokyo, 1994), pp. 26–33.
7. The Usuda tracking station is funded and operated by the Institute of Space and Astronautical Science. The other four tracking stations are funded by NASA, with the Green Bank tracking station being operated by NRAO and the remainder by the Jet Propulsion Laboratory.
8. T.-H. You, J. Ellis, N. Mottinger, *AAS/GSFC International Symposium on Space Flight Dynamics*, American Astronautical Society/Goddard Space Flight Center, Greenbelt, MD, 11 to 15 May 1998 (Univelt, San Diego, CA, in press).
9. M. Schmidt, *Astrophys. J.* **195**, 253 (1974).
10. Redshifts are measured at optical wavelengths by identifying spectral lines and by comparing the observed wavelength to the known emission wavelength;  $\lambda_{\text{observed}} = \lambda_{\text{emitted}} (1 + z)$ , where  $z$  is the redshift. Assuming that the redshift is due to the expansion of the universe, the redshift can be related to the distance from the source. The distances in this paper have been calculated with a value for Hubble's constant  $H$ , which is the expansion rate of the universe, of  $75 \text{ km s}^{-1} \text{ Mpc}^{-1}$  (where 1 Mpc = 3.26 million light-years) and a cosmological deceleration constant of 0.5.
11. J. A. Zensus, *Annu. Rev. Astron. Astrophys.* **35**, 607 (1997).
12. Radiation from a body that is moving relativistically toward the observer is significantly enhanced, an effect known as Doppler boosting. The Doppler factor  $\delta$  is a fundamental parameter describing relativistic motion;  $\delta = [\gamma(1 - \beta \cos \phi)]^{-1}$ , where  $\beta$  is the speed in units of the speed of light,  $\gamma = (1 - \beta^2)^{-1/2}$ , and  $\phi$  is the angle between the line of sight and the radio jet axis.
13. B. G. Piner and K. A. Kingham, *Astrophys. J.* **485**, L61 (1997).
14. R. Mukherjee et al., *ibid.* **490**, 116 (1997).
15. G. A. Moellenbrock et al., *Astron. J.* **111**, 2174 (1996).
16. I. I. Kellermann and I. I. K. Pauliny-Toth, *Astrophys. J.* **155**, L71 (1969).
17. G. L. White et al., *ibid.* **327**, 561 (1988).
18. E. B. Fomalont et al., in preparation.
19. K. I. Kellermann, R. C. Vermuelen, J. A. Zensus, M. H. Cohen, *Astron. J.* **115**, 1295 (1998).
20. P. Charlot, *Astron. Astrophys.* **229**, 51 (1990).
21. A. P. Marscher, Y. F. Zhang, D. B. Shaffer, H. D. Aller, M. F. Aller, *Astrophys. J.* **371**, 491 (1991).
22. P. A. Hughes, H. D. Aller, M. F. Aller, *ibid.* **341**, 54 (1989).
23. H. Kühr, J. W. Liebert, P. A. Strittmatter, G. D. Schmidt, C. Mackay, *ibid.* **275**, L33 (1983).
24. M. Cappi et al., *ibid.* **478**, 492 (1997).
25. K. M. Lanzetta, A. M. Wolfe, D. A. Turnshek, *ibid.* **440**, 435 (1995).
26. G. B. Taylor et al., *Astrophys. J. Suppl. Ser.* **95**, 345 (1994); A. L. Fey and P. Charlot, *ibid.* **111**, 95 (1997).
27. L. I. Gurvits et al., in preparation.
28. C. R. Lawrence, T. J. Pearson, A. C. S. Readhead, S. C. Unwin, *Astron. J.* **91**, 494 (1986).
29. A. Witzel et al., *Astron. Astrophys.* **206**, 245 (1988).
30. T. J. Pearson and A. C. S. Readhead, *Astrophys. J.* **328**, 114 (1988); A. L. Fey, A. W. Clegg, E. B. Fomalont, *Astrophys. J. Suppl. Ser.* **105**, 299 (1996).
31. J. D. Romney et al., *Proc. Natl. Acad. Sci. U.S.A.* **92**, 11360 (1995).
32. R. P. Linfield et al., *Astrophys. J.* **336**, 1105 (1989); R. P. Linfield et al., *ibid.* **358**, 350 (1990).
33. A. C. S. Readhead, *ibid.* **426**, 51 (1994).
34. We thank the many individuals, organizations, and institutions that have made this mission possible and have contributed toward its success. In particular, the support of M. Oda and T. Nishimura in the early stages of the mission is gratefully acknowledged.

5 June 1998; accepted 3 August 1998

# POWERSURGE

**NEW! Science Online's Content Alert Service:** Knowledge is power, and there's only one source that delivers both: *Science's* Content Alert Service. This free enhancement **instantly** e-mails summaries of the latest news and research articles published weekly in *Science*. To sign up for the Content Alert service, go to *Science Online*.

**Science**  
www.sciencemag.org

For more information go to www.sciencemag.org. Click on Subscription button, then click on Content Alert button.